Acta Geodyn. Geomater., Vol. 19, No. 2 (206), 127–142, 2022
DOI: 10.13168/AGG.2022.0003
journal homepage: https://www.irsm.cas.cz/acta

THE EFFECT OF CRACK CHARACTERISTICS ON THE MECHANICAL PROPERTIES AND ENERGY CHARACTERISTICS OF COAL-ROCK COMPOSITE STRUCTURE

Tan LI [1] *, Guangbo CHEN [1], Qinghai LI [2], Bin CAO [2] and Yanhui LI [3]

[1] *Institute of Mining and Coal, Inner Mongolia University of Science and Technology, Baotou, Inner Mongolia, 014010, China*
[2] *College of Energy and Mining Engineering, Shandong University of Science and Technology, Qingdao, Shandong, 266590, China*
[3] *School of Mines, China University of Mining and Technology, Xuzhou 221116, China*

**Corresponding author's e-mail:* litan597@163.com

ARTICLE INFO

Article history:
Received 13 July 2021
Accepted 17 February 2022
Available online 25 February 2022

Keywords:
Crack characteristic
Coal-rock composite structure
Mechanical property
Impact energy index
Sensitivity analysis

ABSTRACT

With the gradual increase of coal mining intensity, many coal pillars need to be left near the stope. The stability of the composite structure of coal pillars and their overlying strata determines the safety of the whole stope and the surface. This paper conducts uniaxial compression tests on coal-rock composite structures with the same lithology and the same coal-rock height ratio and finds the coal-rock composite structure's mechanical properties and failure characteristics have greater discreteness. Combining the CT images of rock and coal, it is concluded that the main reason for the discreteness of the composite structure test results is the different crack characteristics in the rock specimen and the coal specimen. Therefore, this paper uses the PFC numerical simulation software to analyzes the influence of the crack characteristics on the mechanical properties, failure characteristics, and impact energy index of the coal-rock composite structure. The sensitivity factors are used to analyze the influence of crack angle, crack length, crack number and crack position on the peak stress, total crack number, and impact energy index of the coal-rock composite structure. The research results can provide a theoretical basis and guidance for preventing the instability and failure of the coal pillar-roof composite structure.

1. INTRODUCTION

To ensure the safety and efficient mining of coal resources, many coal pillars need to be reserved, such as isolation coal pillars, section coal pillars, waterproof coal pillars, fault protection coal pillars (Frith and Reed, 2018; Wang et al., 2019; Li et al., 2021). These reserved coal pillars play the role of natural support, boundary, and isolation. The stability of the coal-rock composite structure composed of coal pillar and roof determines the safety of the entire stope, the overlying rock, and even the surface. There are many natural cracks in the coal-rock composite structure (as shown in Fig.1), which has an important impact on the stability of the composite structure (Ghasemi et al., 2019; Zhu and Yu, 2020; Sharafisafa et al., 2020). The occurrence of cracks in the rock mass is random, and the mechanical properties of cracks in different parts of the same rock mass are different (Shirole et al., 2020; Liu et al., 2020; Du et al., 2020; Zhou et al., 2020). A large number of studies and practices show that cracks change the mechanical properties of rock mass and change the process of

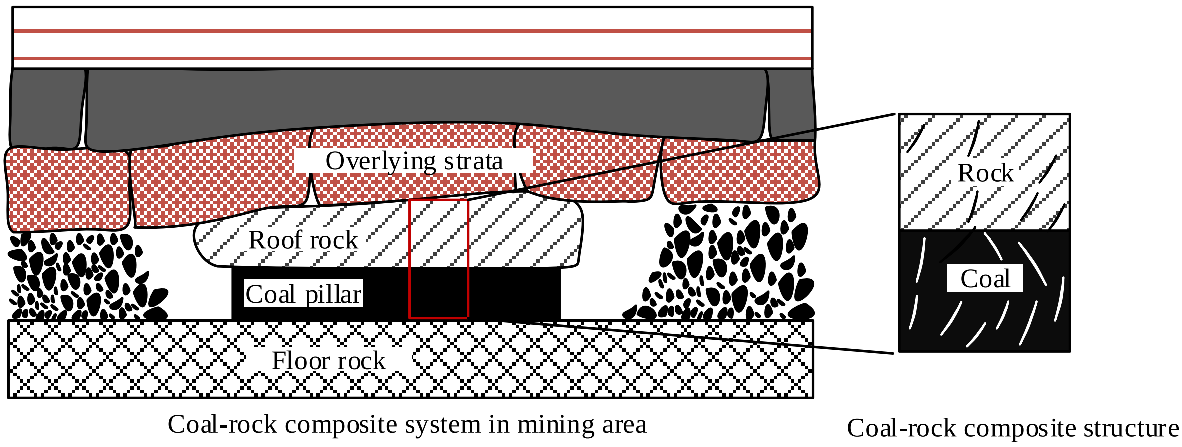

Fig. 1 Schematic diagram of coal-rock composite structure.

Cite this article as: Li T, Chen G, Li Q, Cao B, Li Y: The effect of crack characteristics on the mechanical properties and energy characteristics of coal-rock composite structure. Acta Geodyn. Geomater., 19, No. 2 (206), 127–142, 2022.
DOI: 10.13168/AGG.2022.0003

energy storage and release (Luo et al., 2020; Zhang et al., 2020; Bain et al., 2021). The essence of many dynamic disaster accidents in the coal mine is caused by crack propagation and coalescence under the influence of engineering activities (Wang et al., 2014; Wang et al., 2018; Chen et al., 2020).

For many years, cracked rock mass has been difficult in academic research and the focus of engineering construction (Li et al., 2021). Scholars have carried out a large number of experimental studies on cracked rock mass. (Bulloch, 1992; Eppes et al., 2018; Xu and Li, 2019; Ghasemi et al., 2019; Lin et al., 2021). Liu et al. (2020) study of crack evolution characteristics using acoustic emission (AE) and charge-coupled device camera (CCD camera). They have found that the physical properties and stress boundary of rock influence the cracked state, and the normal force is positively related to the crack geometry. Wong et al. (2014) and Jin et al. (2017) carried out uniaxial loading on rock specimens with a single crack and studied the strength, crack initiation and propagation mode, and ultimate failure mode. Chen and Liu (2015) studied the crack propagation and evolution law of rocks with different fissure dips and different rock bridge dips (β=0°, 30°, 45°, 60°, 90°; α=45°) by numerical tests. Liu et al. (2017) combined numerical simulation and acoustic emission events to explore the strength characteristics, acoustic emission event distribution, and crack initiation and propagation mode of pre-cracked brittle materials. Yang et al. (2017) systematically studied the stress-strain, elastic modulus, and crack initiation and propagation mode of sandstone with double elliptical cracks under different arrangements. Zhang et al. (2021) carried out the uniaxial compression tests to investigate the effect of the joint arrangement on the strength and crack propagation of red sandstone containing a set of preexisting infilled flaws of the same sizes and angles, while AE and strain monitoring observed the crack fracturing process.

A lot of experimental research shows that coal is the first destruction body in the coal-rock composite structure, and coal plays a leading role in the coal-rock composite structure. Therefore, the study of the influence of different crack characteristics on the mechanical properties and impact energy index of the coal-rock composite structure can provide a theoretical basis for preventing the progressive instability of coal pillar and roof composite structure and the failure of roadway surrounding rock. These research conclusions are important and valuable for understanding the crack mechanism of rock engineering in deep underground mining excavations.

2. TEST SYSTEM AND RESULT ANALYSIS

The connection modes of coal pillar and roof strata mainly include the following three types: (1) The coal pillar and its roof strata are bonded as a whole, and there is a cohesive force at the coal rock interface. (2) The coal pillar and its roof strata are freely combined as a whole, and the interface between rock and coal is a bedding plane, there is no cohesive force. (3) The coal pillar and its roof strata are not directly connected as a whole, and the rock coal interface is filled with other materials, such as weak interlayer. This paper mainly studies the mechanical properties of the composite structure of coal pillar and roof rock closely bonded, so the rock specimen and the coal specimen are bonded together during the experiment.

2.1. TEST SYSTEM

The coal and rock samples used in the test were taken from Xin'an Coal Mine, Heilongjiang Province, China. Firstly, a cylinder with a diameter of 50 mm is drilled from coal and coarse sandstone with a coring machine, and then the cylinder is cut into specimens with a height of 50 mm with a cutting machine; then the upper and lower end faces of the specimen are polished with a grinding machine to meet the test requirements. The coal and coarse sandstone are bonded with AB glue to form a standard sample with the coal-rock height ratio of 1:1 (φ 50 mm × 100 mm). The test system of this test mainly includes coal and rock CT scanning system, electro-hydraulic servo pressure control system, and digital video camera system (DVC system), as shown in Figure 2. During the test, the electro-hydraulic servo pressure control system and digital video camera system (DVC system) are synchronized to ensure that the system has the same time parameters. According to the measurement of uniaxial compressive strength in part 7 of “measurement methods for physical and mechanical properties of coal and rock”, the uniaxial compression deformation test is carried out on the specimen, and the loading speed is 0.005 mm/s until the specimen is unstable (Wang and Tan, 2014).

2.2. CT IMAGE

Before the test, the coal and rock samples in the coal-rock composite structure were scanned by CT to observe the distribution of internal cracks. The accuracy of CT scanning can reach 0.1 mm.

Figure 3 is the CT scanning image of the rock specimen in the coal-rock composite structure. It can be seen from the figure that there are no cracks and pores in the rock sample, and the texture is relatively uniform.

Figure 4 is the CT scanning image of the coal specimen in the coal-rock composite structure. It can be seen from Figure 4 (a) that two long cracks are extending on the surface of No. 1 and No. 2 coal samples. There is a long crack along the edge of No. 3 and No. 4 coal samples and a short crack on the surface of No. 5 coal samples. It can be seen from Figure 4 (b) that there is a long crack on the left side of the No. 1 coal sample. There are two parallel cracks on the left side of the No. 2 coal sample and one inclined crack in the middle. There is a horizontal and long crack gap in the No. 3 coal sample, but neither side of the crack extends to the sample surface. There is a long vertical downward crack and a short inclined crack in the No. 4

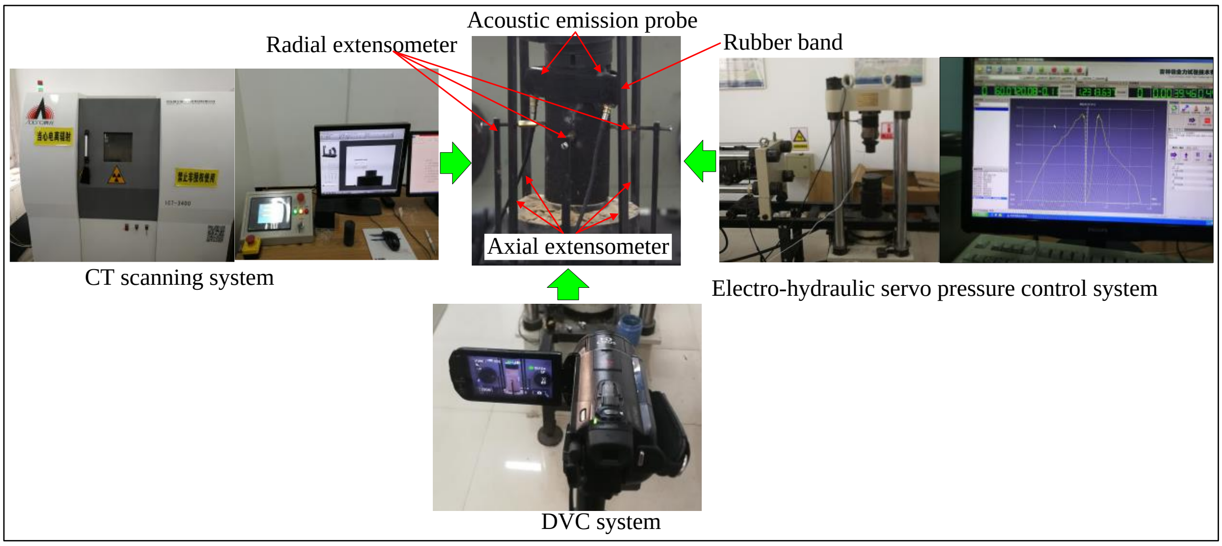

Fig. 2 Test systém.

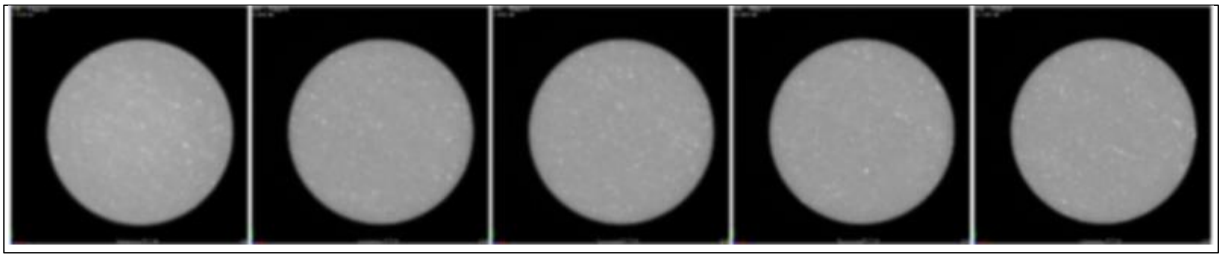

a) Top view

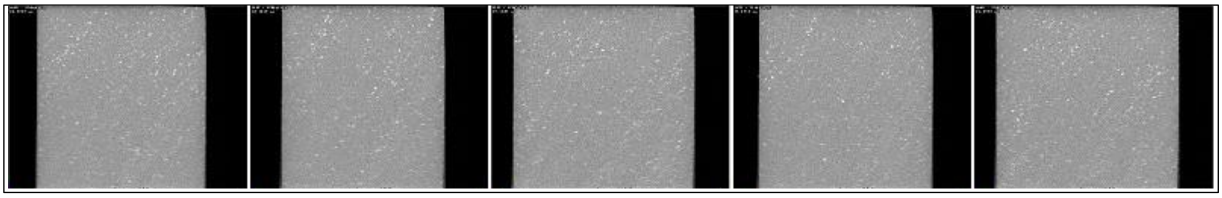

(b) Profile

Fig. 3 CT scanning image of rock specimen.

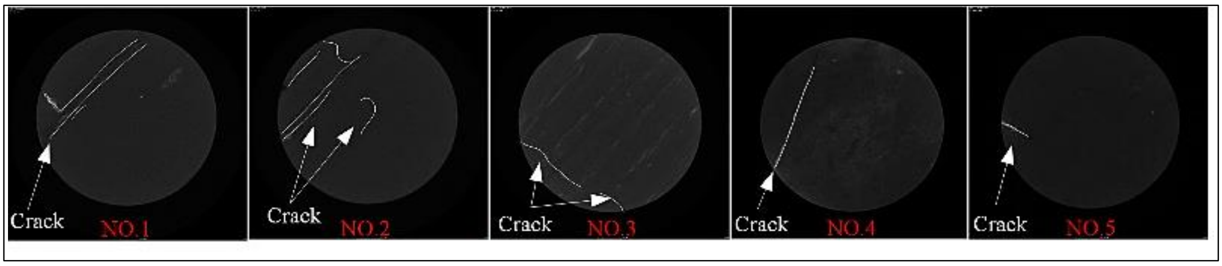

a) Top view

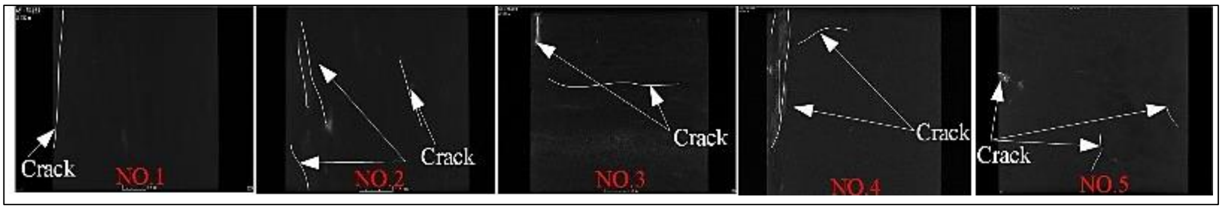

(b) Profile

Fig. 4 CT scanning image of coal specimen.

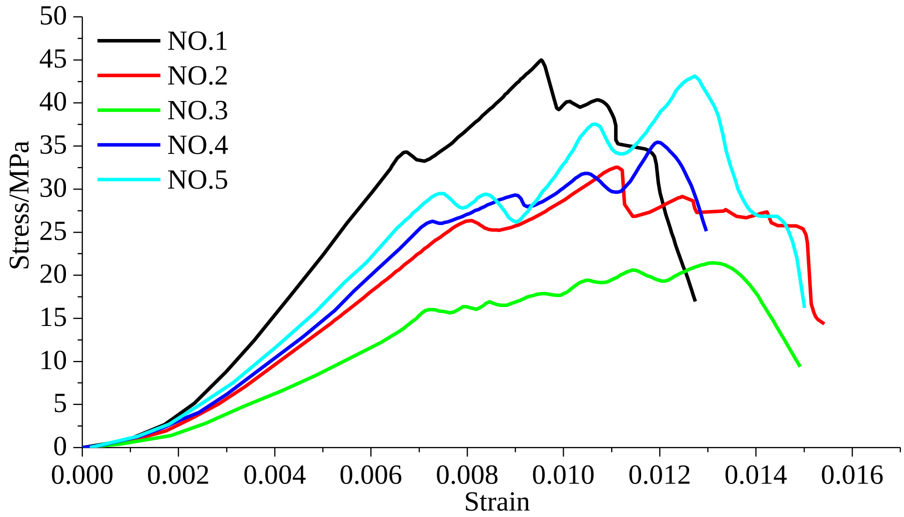

Fig. 5 Stress-strain curve of coal-rock composite structure.

Table 1 Dispersion coefficient of coal-rock composite structure.

	Range	Standard deviation	Average value	Dispersion coefficient (%)
Peak strain	0.0027	0.0011	0.014	7.90
Peak stress	23.55	8.43	35.50	23.73

coal sample, and the long crack extends downward from the top of the sample to the left side of the sample. There are three small cracks in the No. 5 coal sample; the short crack is on the sample's surface and does not extend to the inside of the sample; the other two cracks are vertically distributed inside the sample.

2.3. STRESS-STRAIN CURVE

Figure 5 is the stress-strain curve of the coal-rock composite structure with the same coal-rock height ratio. It can be seen that under the same coal-rock height ratio and the same test conditions, the coal-rock composite structure produces different stress-strain curves. The maximum peak stress is 44.98 MPa, and the smallest is 21.43 Mpa, the difference between them is 23.55 MPa, the maximum peak strain is 0.01542, the smallest is 0.01274, the difference between them is 0.00268.

The dispersion coefficients of the peak strain and peak stress for different coal-rock composite structures are shown in Table 1. The dispersion coefficient of the peak strain and peak stress of coal-rock composite structure with the same lithology and the same coal-rock height ratio is 7.90 % and 23.73 %, respectively under the same test conditions. The differences among different coal-rock composite structures are obvious.

Figure 6 shows the failure state of the coal-rock composite structure. The composite structure with the same lithology and the same coal-rock height ratio produces different failure state. It is mainly because of different crack characteristics in coal-rock composite structure. The composite structures with different crack characteristics produce different crack propagation directions under uniaxial compression, and different crack propagation leads to different failure characteristics of the composite structure.

The coal-rock composite structure is mainly splitting failure. The coal specimen is mainly subject to axial splitting failure, accompanied by spalling, coal wall bulge, and other phenomena. The rock specimen is mainly subject to failure at the coal rock interface, extending from the coal rock interface to the interior of the rock specimen, forming splitting failure or spalling. The failure of coal samples is caused by many crack propagation and penetration. The coal body is the first crack body in compression, which is the main factor in controlling the stability of the coal-rock composite structure. According to the analysis of failure mode and crack initiation position of rock, the main reason for rock failure may be caused by rapid crack propagation and sudden release of elastic energy in coal sample, which is energy-driven instability failure.

Based on the above analysis, it can be concluded that the differences in mechanical properties and failure characteristics of coal-rock composite structure are the distribution of cracks, the density of rock and coal, the form of coal-rock interface. The main reason is the characteristics of primary cracks in the coal-rock composite structure, especially the crack characteristics of coal specimens in the composite structure. Therefore, it is of great significance to study the influence of the crack characteristic on the mechanical properties, energy accumulation, and dissipation of coal-rock composite structures.

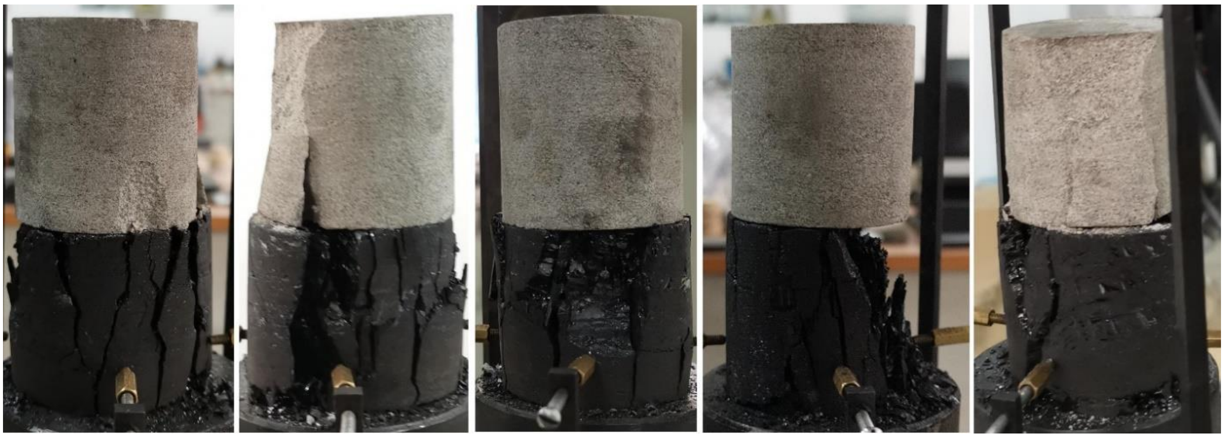

Fig. 6 Failure characteristics of coal-rock composite structure.

3. NUMERICAL SIMULATION

3.1. PARAMETER SELECTION

Rock is composed of the microparticle, and there is a certain bond strength between the microparticle (Dehghan and Mohammadi, 2016; Zhou et al., 2017; Liu et al., 2019). PFC is a numerical analysis software based on discrete elements, studying macro mechanics from microparticles. The medium in PFC numerical simulation software is composed of rigid particles, which are connected by cohesive contact. The cohesive contact between rigid particles is broken and separated from each other, which can simulate the generation and propagation of cracks in the medium. PFC simulation software is suitable for analyzing the meso characteristics (crack cracking, crack penetration) in the process of progressive failure of rock. It can reflect the macroscopic mechanical behavior of rock in essence and can make up for the defect that it is impossible to study the mesoscopic characteristics in laboratory tests. PFC has been widely used to research rock crack and crack propagation (Lisjak and Grasselli, 2014; Chen et al., 2020).

There are three contact modes between particles: pure friction model, contact bonding model, and parallel bonding model in the PFC simulation software (Hadjigeorgiou et al., 2008; Filgueira et al., 2017). In this paper, the parallel bond model is selected, mainly because the parallel bond model can transfer the force and the bending moment, which can better simulate the rock and coal. Therefore, the PFC simulation software was used to simulate the mechanical properties and failure characteristic of coal-rock composite structures with different crack characteristics.

The reasonable setting of micro-mechanical parameters directly determines the matching degree between numerical simulation and experiment results. The micro-mechanical parameters are obtained by constantly adjusting the micro-mechanical parameters according to the stress-strain curve and macroscopic failure state of the rock specimens, to minimize the error between the simulation results and the experiment results.

Through the continuous adjustment of the microscopic parameters of coal and rock in the PFC numerical simulation, the numerical simulation results of coal and rock are very close to the laboratory results, and the microscopic parameters of the PFC numerical simulation of coal and rock can be met the accuracy requirements of the simulation experiment. The results of CT scan images, numerical simulation and experimental comparison of coal and rock are shown in Figures 7-8. It can be seen from the figure that the stress-strain curve of the numerical simulation of coal and rock is similar to the experimental stress-strain curve, and the curve changes are relatively close. The failure modes of coal and rock samples are also similar, indicating that the PFC microscopic parameters of coal and rock meet the experimental requirements.

According to the stress-strain curve and macro failure characteristics of standard coal and rock, the micromechanical parameters of rock and coal are obtained by continuously adjusting the micro parameters to minimize the error between simulation results and test. The microparticle parameters of rock and coal are shown in Table 2.

3.2. NUMERICAL SIMULATION SCHEME

According to the failure mode of the coal-rock composite structure, the coal-rock composite structure with the same lithology and the same coal-rock height ratio has different failure modes under the same loading path. The main reason is the influence of different crack characteristics in the coal-rock composite structure on the composite structure. Based on the above research, the PFC numerical simulation is used to study the influence of different crack characteristics (crack angle, crack length, crack number, and crack position) on the mechanical properties of the coal-rock composite structure. The scheme is shown in Table 3.

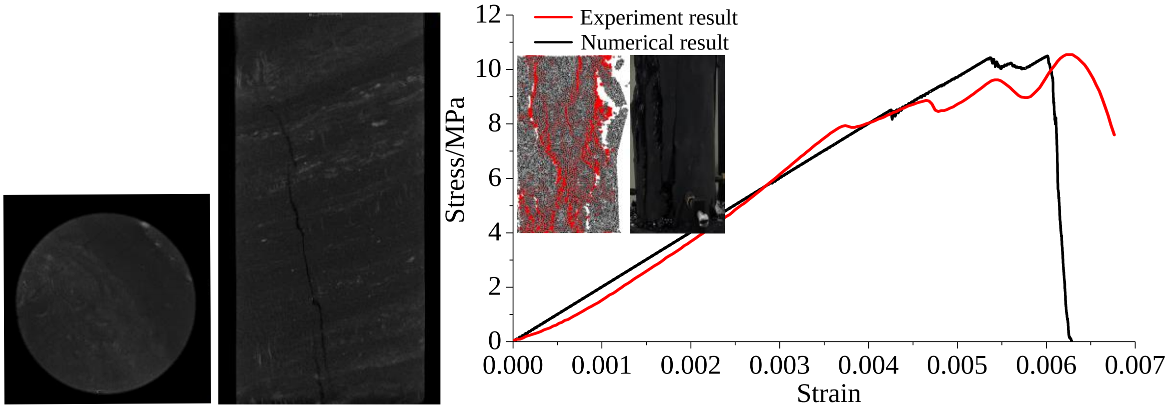

(a) CT image of coal (b) Experiment results of coal

Fig. 7 CT image and experiment results of coal.

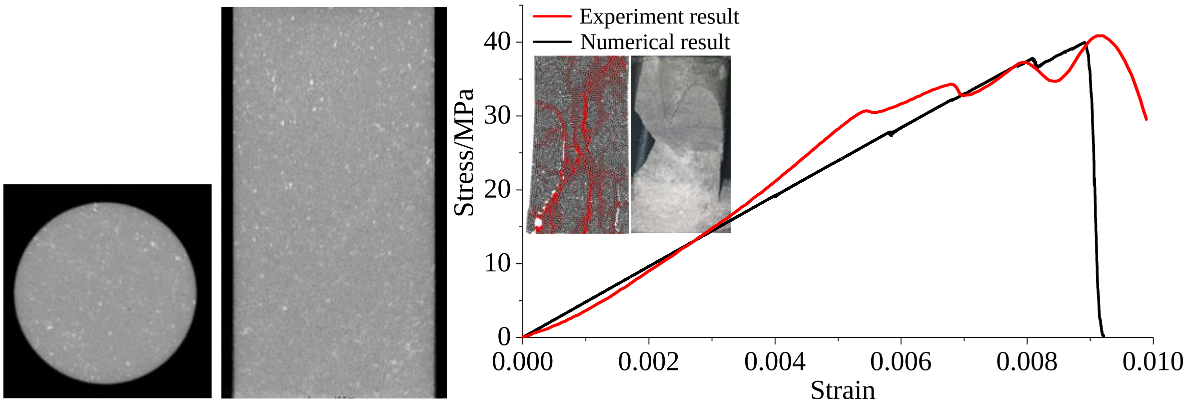

(a) CT image of rock (b) Experiment results of rock

Fig. 8 CT image and experiment results of rosk.

Table 2 Mechanical parameters of rock and coal.

Meso parameters	Rock	Coal
Particle density /(kg·m^{-3})	2600	1800
Radius range /mm	0.2~0.3	0.2~0.3
friction coefficient	0.17	0.15
Contact modulus /GPa	12	3
Parallel bond modulus /GPa	13	4
Parallel bond normal / tangential strength /MPa	45	16
Parallel bond normal / tangential stiffness	3.2	2.1
Parallel bond radius value	1	1

Table 3 Numerical simulation scheme of different fracture characteristics.

Scheme	Crack angle/°	Crack length/m	Crack number	Distance from crack center to bottom /m
1	15°、45°、75°	0.025	1	0.025
2	45°	0.015、0.025、0.035	1	0.025
3	45°	0.025	1、2、3	0.025
4	45°	0.025	1	0.0088、0.025 、0.412

There are relatively few cracks in the rock and more cracks in the coal specimen through the CT image, so the cracks are set in the coal specimen. The model size of the composite structure is 50 mm × 100 mm, the upper part of the model is rock, the lower part is coal, and the coal-rock height ratio is 1:1. The numerical simulation model is shown in Figure 9.

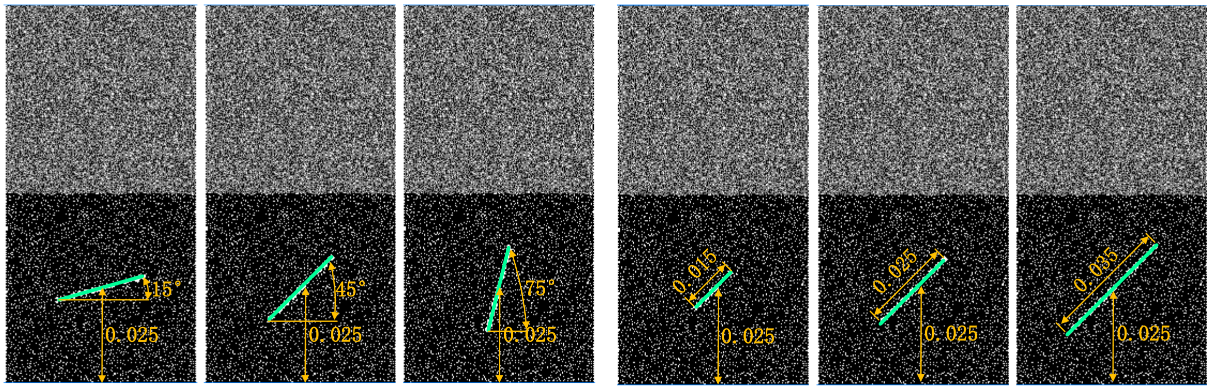

a) Different crack angles (b) Different crack lengths

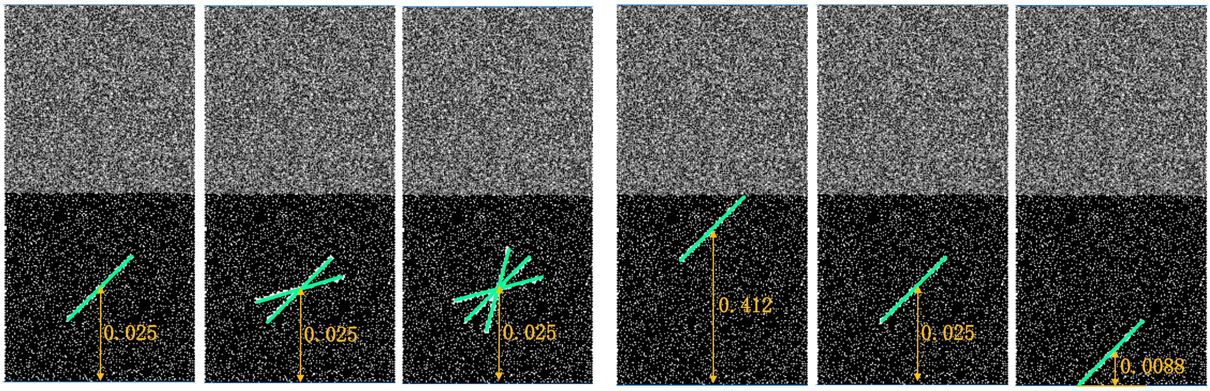

(c) Number of different crack (d)Different crack positions

Fig. 9 The numerical simulation model.

3.3. INFLUENCE OF CRACK CHARACTERISTICS ON STRENGTH AND FAILURE CHARACTERISTICS

The numerical simulation results of composite structures with different crack characteristics are shown in Figures 10-13. Under the action of stress, the crack tip produces concentrated stress. When the concentrated stress exceeds the strength of the material, the crack begins to propagate towards the direction of the principal stress, making the crack direction parallel or nearly parallel to the principal stress direction when the specimen finally destroys. The failure degree of coal specimen is large, accompanied by coal wall bulge, spalling, and even the outward ejection of broken blocks. The failure of rock specimens in a composite structure is mainly due to the expansion of cracks in coal specimens to rock specimens, forming large through cracks or splitting failure along the principal stress direction.

It can be seen from Figure 10 that the smaller the pre-existing crack angle is, the deeper the crack extends to the rock specimen, which penetrates from the coal-rock interface to the top of the rock specimen. When the pre-existing crack angle is 75 °, the crack extends about 0.02 mm upward from the coal-rock interface. The peak stress is the lowest when the pre-existing crack angle is 45 °, indicating that when the dip angle between axial stress and pre-existing crack is 45°, it is more conducive to the expansion of the crack, and the peak stress of the composite structure is lower.

It can be seen from Figure 11 that the smaller the pre-existing crack length is, the deeper the crack extends to the rock specimen, which penetrates from the coal-rock interface to the top of the rock specimen. Because the smaller the crack length is, the smaller the guiding effect of the crack outward expansion under stress is, the more divergent the direction of the crack outward expansion is, and the larger the damage scope and degree are formed. The crack expansion direction is roughly along the axial stress direction. The larger the pre-existing crack length is, the lower the peak stress is. When the crack length increases from 0.015 mm to 0.035 mm, the peak stress decreases by 54.13 %.

It can be seen from Figure 12 that the more the number of pre-existing cracks, the greater the damage degree of the composite structure, the more the cracks at the crack tip, the deeper the crack extends to the rock specimen. The more the number of pre-existing cracks, the lower the peak stress of the composite structure. When the number of pre-existing cracks increases from 1 to 3, the stress decreases by 53.36 %.

It can be seen from Figure 13 that when the angle, length, and the number of pre-existing cracks are

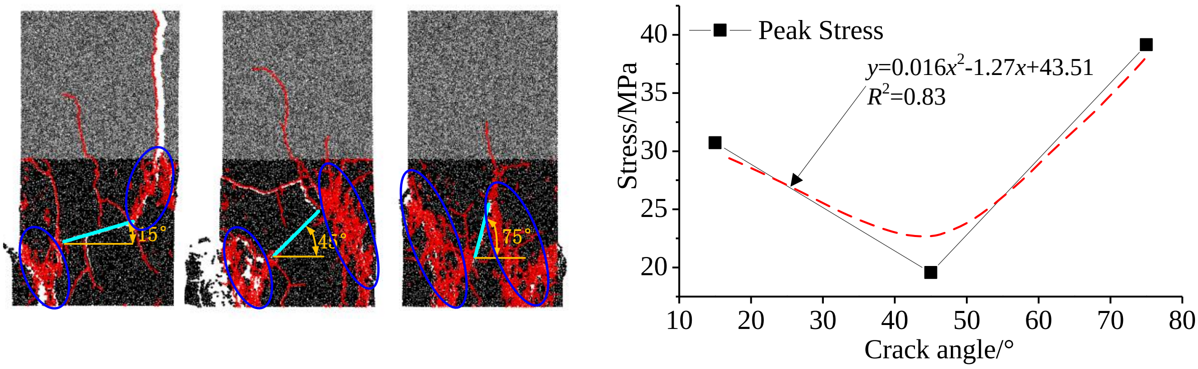

(a) Failure characteristics (b) Curve of stress-crack angles

Fig. 10 Experiment results of different crack angles.

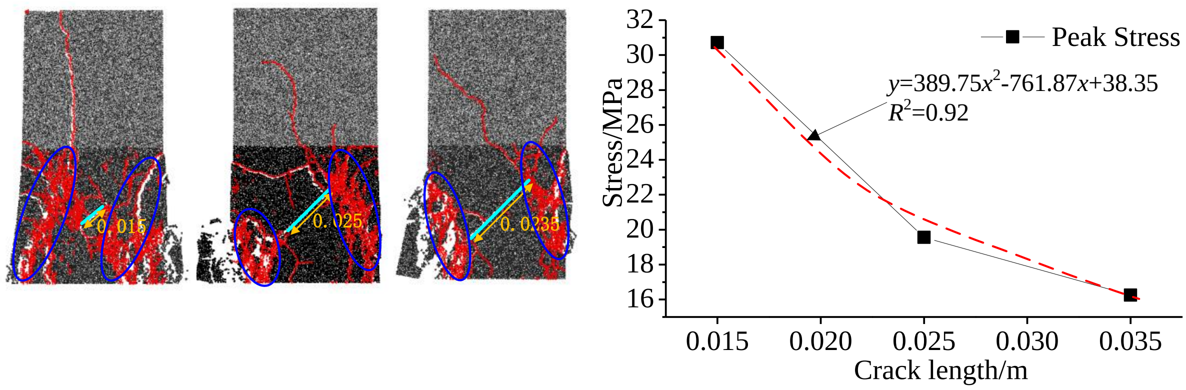

(a) Failure characteristics (b) Curve of stress-crack lengths

Fig. 11 Experiment results of different crack lengths.

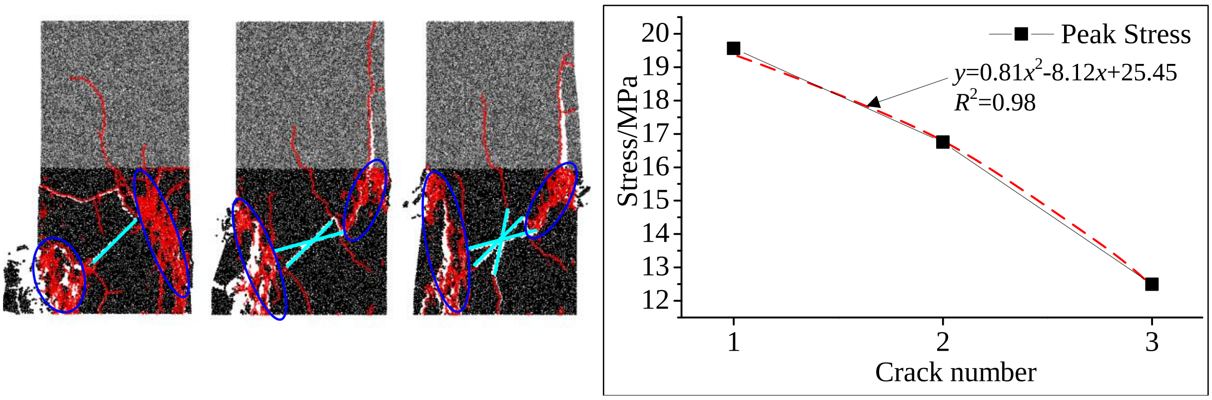

(a) Failure characteristics (b) Curve of stress-crack numbers

Fig. 12 Experiment results of different crack numbers.

fixed, the farther the distance between the position of the pre-existing crack and the bottom of the composite structure, the more cracks are generated in the composite structure. With the increase of the distance between the pre-existing cracks and the bottom of the coal-rock composite structure, the peak stress increases.

3.4. *THE INFLUENCE OF CRACK CHARACTERISTICS ON THE NUMBER OF CRACKS*

The number of cracks in the compression process of rock specimens with different crack characteristics is calculated, and the results are shown in Figure14. With the increase of loading steps, the cracks generated in the composite structure grow in steps. The main reason is that the crack propagation is driven by energy. When the energy gathered at the crack tip

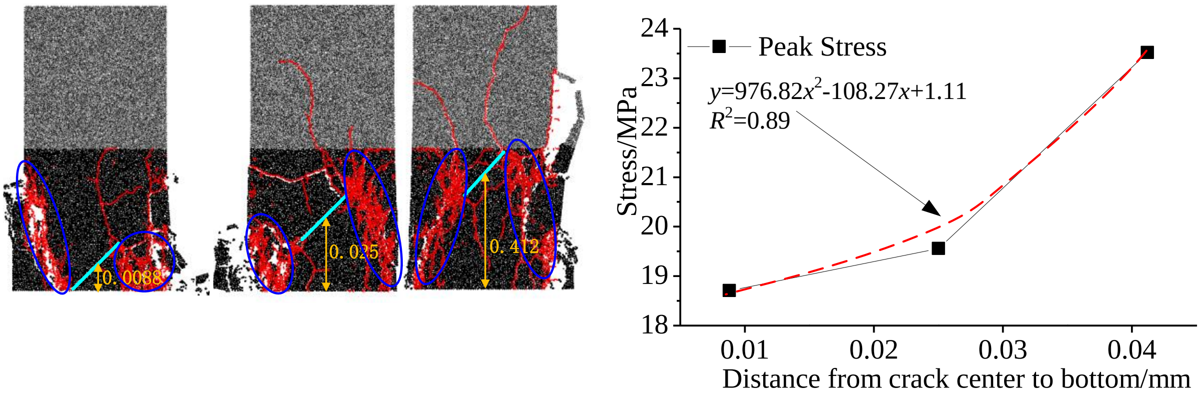

(a) Failure characteristics (b) Curve of stress-crack position

Fig. 13 Experiment results of different crack position.

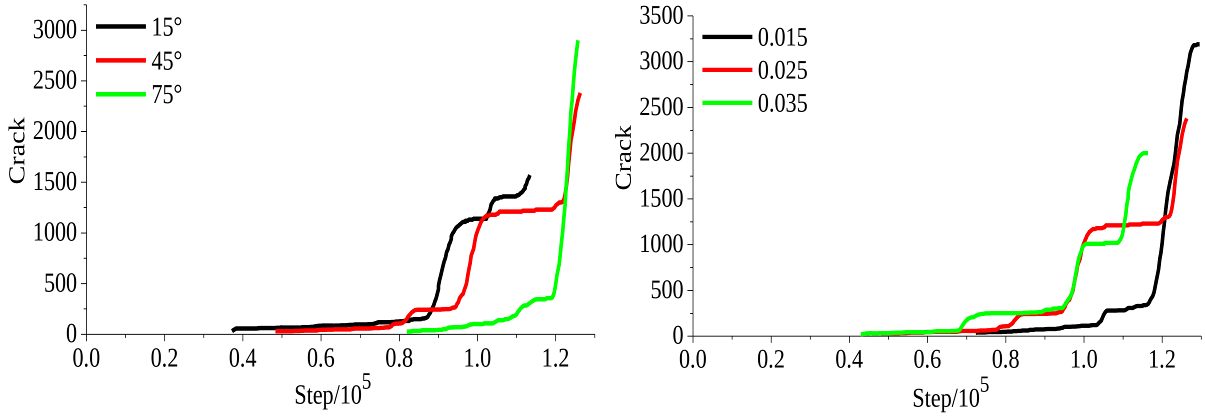

(a) Angle (b) Length

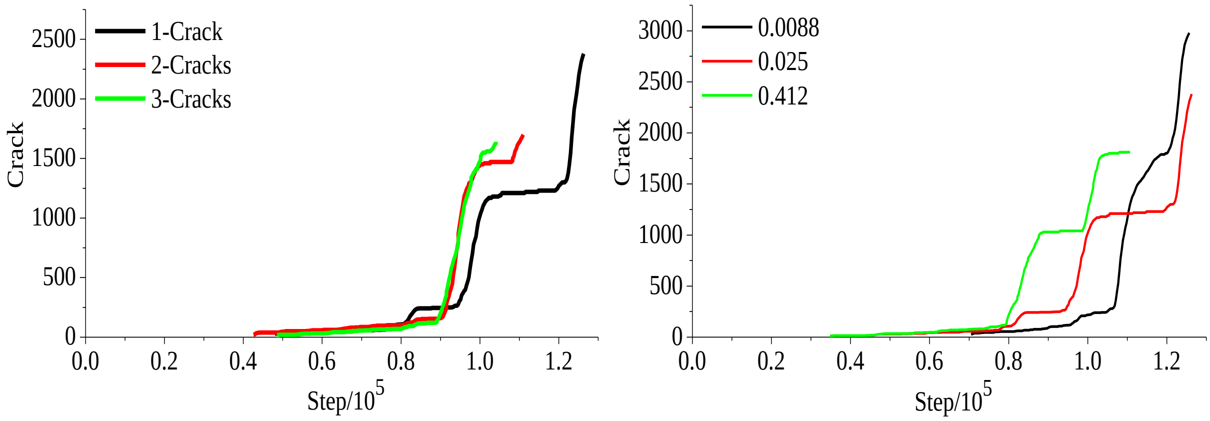

(c) Number (d) Position

Fig. 14 Variation curve of crack.

meets the requirements of crack propagation, the crack expands. At the initial stage of loading of coal-rock composite structure, the pores and cracks in the rock samples are gradually compacted, no cracks are produced in this process. With the increase of stress, the crack tip and the fragile part of the specimen first meet the crack propagation conditions, and the cracks expand or produce small cracks, the cracks increases. With the development and expansion of small cracks, small cracks are gradually connected to form larger cracks, the cracks increases again. Large cracks continue to expand and develop, forming large macroscopic cracks, the phenomenon of specimen cracking, sidewall and spalling appears, the cracks increases sharply.

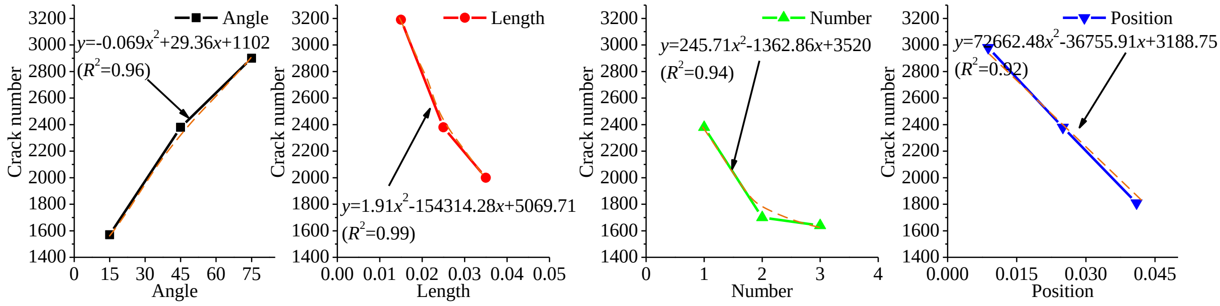

Fig. 15 Variation curve of total cracks.

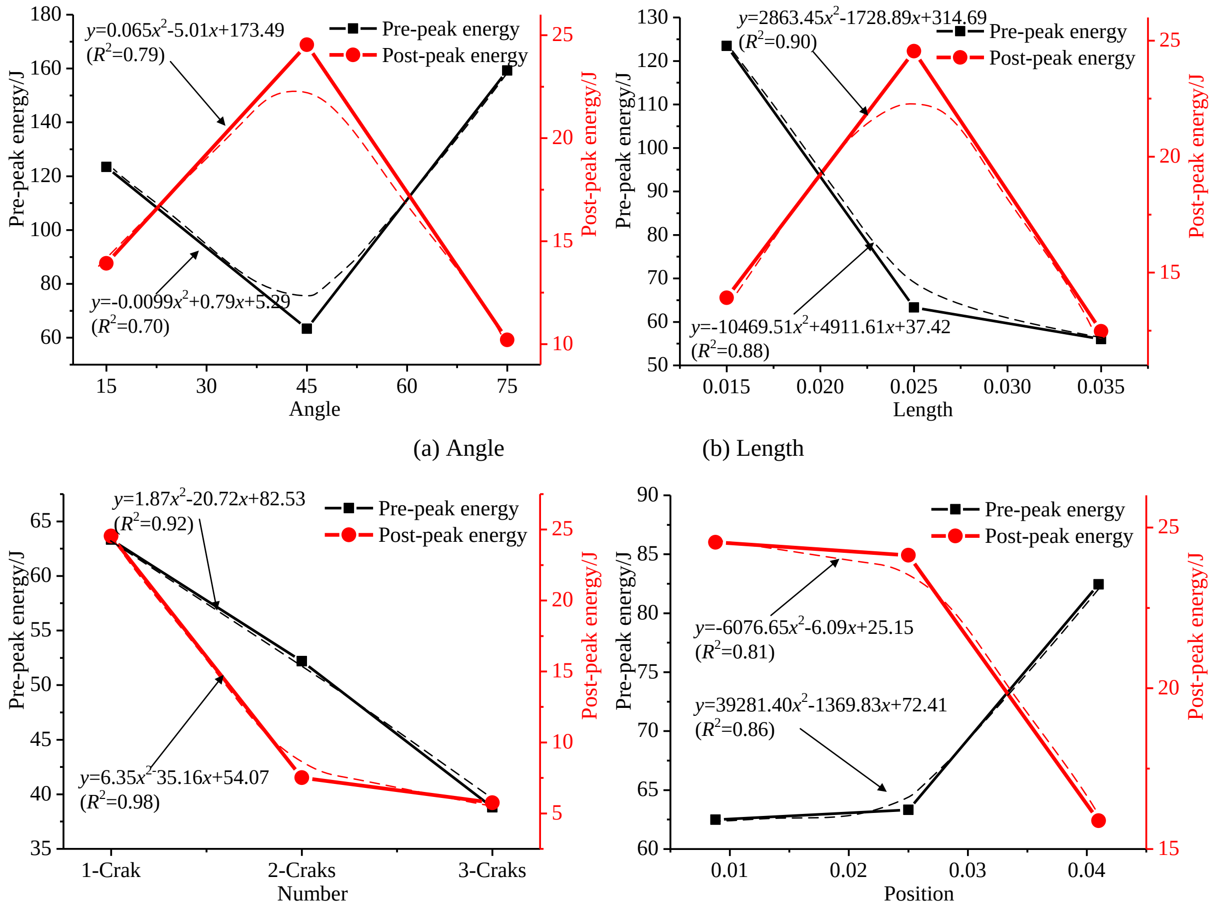

(a) Angle (b) Length

(c) Number (d) Position

Fig. 16 Pre-peak energy and post-peak energy.

Figure 15 shows the variation curve of total cracks in the coal-rock composite structure with different crack characteristics. It can be seen that during the compression process, the number of cracks is directly proportional to the angle of pre-existing cracks and inversely proportional to the length, number, and distance from the crack to the bottom of pre-existing cracks. Because the larger the crack angle is, the smaller the angle between the crack and the stress is, the smaller the component force generated in the direction of crack expansion is, and the more time the crack expands outward under the action of stress, the more cracks are generated. The larger the length, number, and distance from crack to bottom, the stronger the non-uniformity of rock specimen, the lower the peak stress, the shorter the time of crack propagation, and the less the crack number.

4. IMPACT ENERGY INDEX

The impact energy index is a kind of inherent property of rock mass. The ratio of accumulated energy before the peak to dissipated energy after the peak is the impact energy index expressed by K_e (Li et al., 2011; Sun et al., 2019). The impact energy index directly and comprehensively reflects the whole process of accumulating and dissipate energy and shows the physical essence of the impact tendency (Halim et al., 2013; Kopacz et al., 2017).

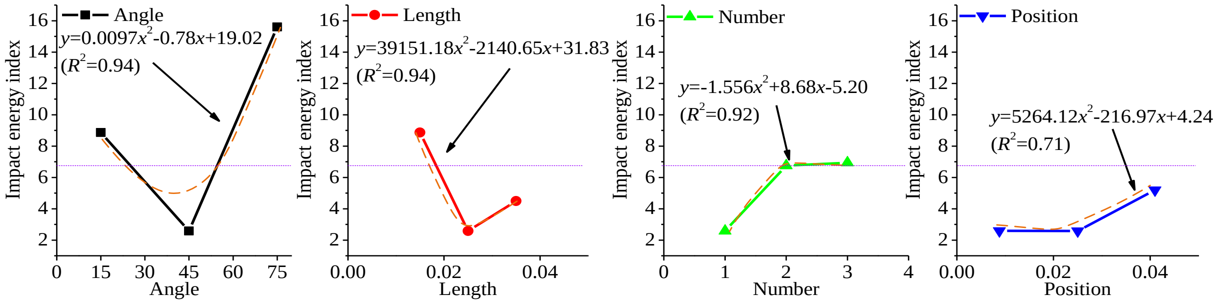

Fig. 17 Impact energy index.

Figure 16 is the variation curves of pre-peak energy and post-peak energy of coal-rock composite structures with different crack characteristics. It can be seen from Figure 16(a) that the pre-peak energy decreases first and then increases with the increase of crack angle, which is the minimum when the crack angle is 45°. The post-peak energy increases first and then decreases with the increase of crack angle, which is the maximum when the crack angle is 45°. It can be seen from Figure 16(b) that the pre-peak energy decreases gradually with the increase of crack length. The post-peak energy increases first and then decreases with the increase of crack length; when the crack length is 0.025 mm, the post-peak energy is the largest. It can be seen from Figure 16(c) that the pre-peak energy and post-peak energy gradually decrease with the increase of the number of cracks. It can be seen from Figure 16(d) that when the crack is located in the middle of the coal-rock composite structure, the pre-peak energy is larger, and the post-peak energy is low.

Based on the above analysis, when the pre-existing crack angle is 45°, the pre-existing crack length is 0.025 mm and the pre-existing crack is in the middle position of coal-rock composite structure, the pre-peak energy is large and the post-peak energy is small. The pre-peak energy and post-peak energy decrease with the increase of crack number.

Figure 17 shows the variation curve of the impact energy index of the coal-rock composite structure with different crack characteristics. The average impact energy index of the coal-rock composite structure obtained in the test is 6.75, as shown by the dotted line in the figure. When the crack angle is 15° and 75°, the crack length is 0.015 mm, and the number of cracks is 3, the impact energy index obtained by numerical simulation is higher than the impact energy index obtained by test. When the pre-existing crack angle is 45 °, and the pre-existing crack length is 0.025 mm, the impact energy index of the coal-rock composite structure is the lowest, which is 2.58.

The impact energy index decreases at first and then increases with the increase of pre-existing crack angle and pre-existing crack length, the impact energy index is the lowest when the pre-existing crack angle is 45 ° and when the pre-existing crack length is 0.025 m. Because the larger the angle between the axial stress and the pre-existing crack is, the easier the crack is to expand, the less the accumulated energy is. When the pre-existing crack length is 0.025 m, the pre-existing crack length has a great guiding effect on the crack propagation, the crack expansion is sufficient, the post-peak energy produced is larger, the smaller the impact energy index is.

The impact energy index increases with the increase of the cracks and the distance from the pre-existing crack to the bottom of the specimen. Because the cracks increases from 2 to 3 and the pre-existing cracks move from the bottom to the middle of the specimen, the influence on the accumulated energy of the composite structure is small, and the change of impact energy index is also small.

The impact energy index increases with the increase of the number of pre-existing cracks. When the number of pre-existing crack increases from 1 to 2, the increased rate of impact energy index is 161.70 %. When the number of pre-existing crack increases from 2 to 3, the increased rate of impact energy index is 2.78 %. The increased rate of impact energy index is greater when the number of pre-existing crack increases from 1 to 2.

When pre-existing crack moves from the bottom of the composite structure to the middle part of the coal specimen, the increase rate of the impact energy index is 0.37 %. When the p position of pre-existing crack moves from the middle part to the upper part of the coal sample, the increase rate of the impact energy index is 50.31 %. The ratio of the increase of the impact energy index is higher when pre-existing crack moves from the middle part to the upper part of the coal specimen.

5. SENSITIVITY ANALYSIS

Sensitivity analysis is a quantitative method to analyze the influence of the input factors of the model on the target value. Sensitivity analysis can find out the sensitive factors of the model, and then increase the control of sensitive factors to achieve the desired goal. Sensitivity analysis can be used to quantitatively

Table 4 Classification of the importance of design parameters.

Parameter classification	Important parameter	Primary parameter	Secondary parameter	Negligible parameter
Sensitive percentage γ_{xi}	[100 %, 50 %]	(50 %, 25 %]	(25 %, 5 %]	(5 %, 0 %]

determine the influence degree of each crack characteristic on the mechanical properties, total crack number, and impact energy index of the composite structure. The greater the sensitivity of crack characteristics, the greater the influence of crack characteristics on the mechanical properties, total crack number and impact energy index of the composite structure.

The basic idea of sensitivity analysis is to fit the analytical expression $z=g(x_1, x_2, x_3, \dots, x_n)$ between a response function Z and the basic variables$(x_1, x_2, x_3, \dots, x_n)$ through a finite number of experiments to replace the actual response function $Z=G(x_1, x_2, x_3, \dots, x_n)$ which can not be expressed clearly. There are two main forms of a response function expression.

One is the quadratic polynomial response function equation with cross terms proposed by Wong (1985):

$$g(x)=a+\sum_{i=1}^{n} b_i x_i+\sum_{i=1}^{n}\sum_{j\leq i}^{n} c_{ij} x_i x_j \quad (1)$$

Where, $x_{ij}(i, j=1, 2, 3, \dots, n)$ is the design variable, a, b_i, $c_{ij}(i, j=1, 2, 3, \dots, n)$ is an undetermined factor.

The other is the quadratic polynomial response function equation without cross term proposed by Bucher and Bourgund (1990):

$$g(x)=d+\sum_{i=1}^{n} e_i x_i+\sum_{i\neq j}^{n} f_j x_j^2 \quad (2)$$

Where, $x_i(i=1, 2, 3, \dots, n)$ is the design variable, d, e_i, $f_j(i, j=1, 2, 3, \dots, n)$ is an undetermined factor.

Because formula (2) does not contain quadratic cross-terms, in the case of the same number of design parameters, the undetermined factor is less than that of formula (1), and the response function equation needs fewer regression iterations, short solving time, and high efficiency. Therefore, this paper uses formula (1) for sensitivity analysis.

The purpose of sensitivity analysis is to understand the sensitivity of the target value to the variation of design parameters. Therefore, this paper uses the dimensionless sensitive factors in system analysis to sort the influencing factors, to distinguish the main parameters and secondary parameters (Castillo et al., 2003; Yu et al., 2016; Patil et al., 2020).

The expression of the sensitivity factor is:

$$S_{x_i}=\left|\frac{dg(x)}{dx}\right|\frac{x_i^*}{g(x_i)^*} \quad (i=1, 2, \dots n) \quad (3)$$

Where: S_{x_i} is the sensitive factor when parameter xi takes the reference value x_i^*; g(x) is the index function of parameter xi; $g(x_i)^*$ is the index value when parameter xi takes the reference value x_i^*.

Therefore, the sensitivity percentage γ_{xi} of a design parameter x_i can be expressed as:

$$\gamma_{x_i}=\left|\frac{S_{x_i}}{\sum_{i=1}^{n} S_{x_i}}\right| \quad (4)$$

In the past, parameter sensitivity analysis generally divided the design parameters into important influence parameters and secondary influence parameters and did not give the basis for the division, which is not conducive to parameter identification and error control. This paper proposes to divide the design parameters into four levels according to the sensitivity percentage: important parameter, primary parameter, secondary parameter, and negligible parameter, as shown in Table 4 (Hu et al., 2021).

The influencing factors are ranked according to the dimensionless sensitive factors. The selected indexes are the peak stress, total crack number, and impact energy index of the coal-rock composite structure. The influencing factors are crack angle, crack length, total crack number, and the distance from the crack center to the bottom of the composite structure.

The relationship of each influencing factors is fitted, the fitting function of peak stress with crack angle, crack length, crack number and crack position is as follows:

$$y=0.016x^2-1.27x+43.51 \quad (R^2=0.83) \quad (5)$$

$$y=389.75x^2-761.87x+38.35 \quad (R^2=0.92) \quad (6)$$

$$y=0.81x^2-8.12x+25.45 \quad (R^2=0.98) \quad (7)$$

$$y=976.82x^2-108.27x+1.11 \quad (R^2=0.89) \quad (8)$$

The fitting function of total crack number with crack angle, crack length, crack number and crack position is as follows:

$$y=-0.069x^2+29.36x+1102 \quad (R^2=0.96) \quad (9)$$

$$y=1.91x^2-154314.28x+5069.71 \quad (R^2=0.99) \quad (10)$$

$$y=245.71x^2-1362.86x+3520 \quad (R^2=0.94) \quad (11)$$

$$y=72662.48x^2-36755.91x+3188.75 \quad (R^2=0.92) \quad (12)$$

The fitting function of impact energy index with crack angle, crack length, crack number and crack position is as follows:

$$y=0.0097x^2-0.78x+19.02 \quad (R^2=0.94) \quad (13)$$

$$y=39151.18x^2-2140.65x+31.83 \quad (R^2=0.94) \quad (14)$$

$$y=-1.56x^2+8.68x-5.20 \quad (R^2=0.92) \quad (15)$$

$$y=5264.12x^2-216.97x+4.24 \quad (R^2=0.71) \quad (16)$$

Table 5 Sensitivity factors.

Influencing factors	Crack angle	Crack length	Crack number	Distance from the crack center to the bottom
Peak stress	0.33	0.95	0.39	0.08
Total crack number	0.42	0.63	0.16	0.38
Impact energy index	1.62	1.77	4.57	0.45

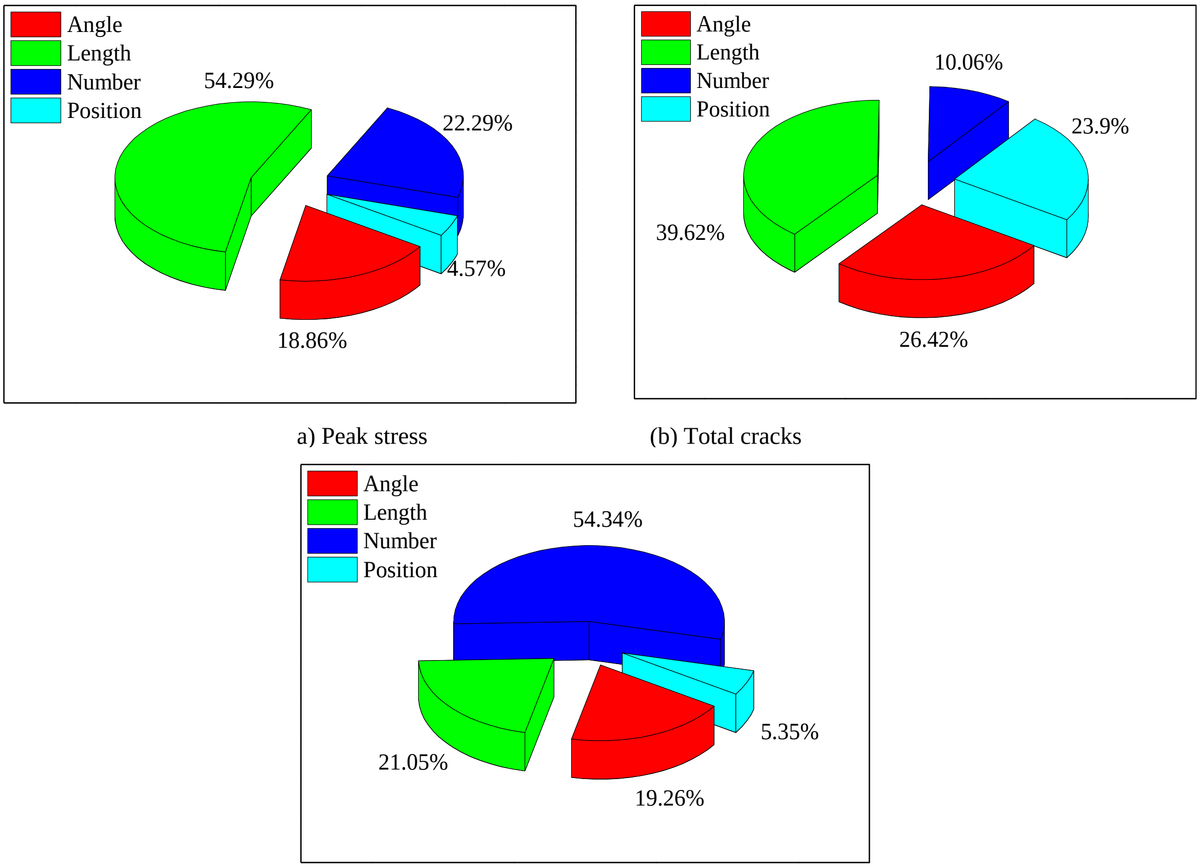

a) Peak stress (b) Total cracks

c) Impact energy index

Fig. 18 Sensitivity percentage.

According to the sensitivity analysis, the sensitivity factors of peak stress, total crack number and impact energy index are shown in Table 5.

For the peak stress of the composite structure, the sensitivity factors of the crack length are the largest, followed by the crack number, and the smallest sensitivity factor is the distance from the crack center to the bottom of the composite structure. It shows that the crack length has a great influence on the peak stress, and the position of the crack in the composite structure has little influence on the peak stress.

For the total crack number of composite structures, the sensitivity factor of the crack length is the largest, followed by crack angle, and the crack number is the smallest. It shows that the crack length greatly influences the total crack number, and the influence of the crack number is small.

For the impact energy index of the composite structure, the sensitivity factor of a crack number is the largest, followed by the crack length, and the minimum sensitivity factor is the distance from the crack center to the bottom of the composite structure. It shows that the crack number has a great influence on the impact energy index, and the position of cracks in the composite structure has little influence on the impact energy index.

Figure 18 shows the sensitivity percentage of different crack characteristics to peak stress, total crack number, and impact energy index. It can be seen that the sensitive percentages of crack angle to peak stress and impact energy index are 18.86 % and 19.26 %, respectively, which are secondary parameters. The sensitive percentage of crack angle to total cracks is 26.42 %, which is a primary parameter.

The sensitive percentages of crack length to peak stress is 54.29 %, which are important parameters. The sensitive percentages of crack length to total cracks is 39.62 %, which are parameter parameters. The sensitive percentage of crack length to impact energy index is 21.05 %, which is a secondary parameter.

The sensitive percentages of the crack number to peak stress and total crack are 22.29 % and 10.06 %, which are secondary parameters. The sensitive percentage of the crack number to impact energy index is 54.34 %, which is an important parameter.

The sensitive percentages of crack position to total crack and impact energy index are 23.90 % and 5.35 %, which are secondary parameters. The sensitive percentage of crack position to peak stress is 4.57 %, which is a negligible parameter.

6. CONCLUSION

1. The dispersion coefficients of the peak strain and peak stress of the coal-rock composite structure with the same lithology and the same coal-rock height ratio under the same loading are 7.90 % and 23.73 %, respectively. Comparing the CT images of rock specimens and coal specimens, it can be concluded that the main reason for the dispersion is the different crack characteristics of coal specimens in the composite structure.
2. The direction of crack expansion is approximately along the principal stress direction. When the angle between the principal stress and pre-existing crack is 45 °, the peak stress of the composite structure is low. The larger the crack length, the greater the guiding effect of the crack outward expansion. The closer the crack is to the coal rock interface, the more cracks are produced in the composite structure, the greater the damage degree.
3. When the pre-existing crack angle is 45°, and the pre-existing crack length is 0.025mm, the pre-peak energy is larger, the post-peak energy is lower, the impact energy index is the lowest. The pre-peak energy and post-peak energy decrease with the increase of crack number.
4. The crack length is the most sensitive to the peak stress and total crack number, and the crack number is the most sensitive to the impact energy index. The sensitivity of crack location to peak stress and impact energy index of the coal-rock composite structure is the least, and the sensitivity of crack number to the total crack number of the coal-rock composite structure is the least.

ACKNOWLEDGEMENTS

This study was supported by the National Natural Science Foundation of China [No. 51604164] and by the Natural Science Foundation of Inner Mongolia (No. 2021LHMS05015).

REFERENCES

Bain, A.A., Kendrick, J.E., Lamur, A., Yan, L. and Torres, R.A.: 2021, Micro-textural controls on magma rheology and vulcanian explosion cyclicity. Front. Earth Sci., 8. DOI: 10.3389/feart.2020.611320

Bucher, C.G. and Bourgund U.A.: 1990, A fast and efficient response surface approach for structural reliability problems. Struct. Saf., 7, 1, 57–66. DOI: 10.1016/0167-4730(90)90012-E

Bulloch, J.H.: 1992, Characteristics of the fatigue crack extension process in quartzite rock. Theor. Appl. Fract. Mech., 17, 93–105. DOI: 10.1016/0167-8442(92)90034-U

Castillo, E., Conejo, A.J., Mínguez, R. and Castillo, C.: 2003, An alternative approach for addressing the failure probability-safety factor method with sensitivity analysis. Reliab. Eng. Syst. Saf., 82, 2, 207–216. DOI: 10.1016/S0951-8320(03)00164-9

Chen, B., Zhang, S., Li, Y., Li, Z. and Zhou, H.: 2020, Physical simulation study of crack propagation and instability information discrimination of rock-like materials with faults. Arab. J. Geosci., 13, 18, 966. DOI: 10.1007/s12517-020-05966-8

Chen, L. and Liu, J.: 2015, Numerical analysis on the crack propagation and failure characteristics of rocks with double fissures under the uniaxial compression. Petroleum, 1, 4, 373–381. DOI: 10.1016/j.petlm.2015.10.009

Chen, S.J., Xia, Z.G., Feng, F. and Yin, D.W.: 2020, Numerical study on strength and failure characteristics of rock samples with different hole defects. Bull. Eng. Geol. Environ., 80, 2, 1523–1540. DOI: 10.1007/s10064-020-01964-y

Dehghan, M. and Mohammadi, V.: 2016, The numerical simulation of the phase field crystal (PFC) and modified phase field crystal (MPFC) models via global and local meshless methods. Comput. Methods Appl. Mech. Eng., 298, 453–484. DOI: 10.1016/j.cma.2015.09.018

Du, K., Li, X.F., Tao, M. and Wang, S.F.: 2020, Experimental study on acoustic emission (AE) characteristics and crack classification during rock fracture in several basic lab tests. Int. J. Rock Mech. Min. Sci., 133, 104411. DOI: 10.1016/j.ijrmms.2020.104411

Eppes, M.C., Hancock, G.S., Chen, X., Arey, J. and Whitten, J.: 2018, Rates of subcritical cracking and long-term rock erosion. Geology, 46, 11, 951–954. DOI: 10.1130/G45256.1

Filgueira, U.C., Alejano, L.R., Arzúa, J. and Ivars, D.M.: 2017, Sensitivity analysis of the micro-parameters used in a PFC analysis towards the mechanical properties of rocks. Procedia Eng., 191, 488–495. DOI: 10.1016/j.proeng.2017.05.208

Frith, R. and Reed, G.: 2018, Coal pillar design when considered a reinforcement problem rather than a suspension problem. Int. J. Min. Sci. Technol., 28, 1, 11–19. DOI: 10.1016/j.ijmst.2017.11.013

Ghasemi, S., Khamehchiyan, M., Taheri, A., Nikudel, M.R. and Zalooli, A.: 2019, Crack evolution in damage stress thresholds in different minerals of granite rock. Rock Mech. Rock Eng., 53, 3, 1163–1178. DOI: 10.1007/s00603-019-01964-9

Hadjigeorgiou, J., Esmaieli, K. and Grenon, M.: 2008, Stability analysis of vertical excavations in hard rock by integrating a fracture system into a PFC model. Tunn. Undergr. Space Technol. incorporating Trenchless Technology Research, 24, 3, 296–308. DOI: 10.1016/j.tust.2008.10.002

Halim, M.A., Majumder, R.K., Zaman, M.N. and Hossain, S.: 2013, Mobility and impact of trace metals in barapukuria coal mining area, northwest bangladesh. Arab. J. Geosci., 6, 12, 4593–4605. DOI: 10.1007/s12517-012-0769-1

Hu, Z.Q., Ma, B., Chen, X.Z. and Tangchirapat, W.C.: 2021, Study on sensitivity parameters analysis of grouting reinforcement underpassing existing subway tunnel by numerical modeling. Adv. Civ. Eng. DOI: 10.1155/2021/8868216

Jin, J., Cao, P., Chen, Y., Pu, C.Z., Mao, D.W. and Fan, X.: 2017, Influence of single flaw on the failure process and energy mechanics of rock-like material. Comput. Geotech., 86, 150–162. DOI: 10.1016/j.compgeo.2017.01.011

Kopacz, M., Kryzia, D. and Kryzia, K.: 2017, Assessment of sustainable development of hard coal mining industry in Poland with use of bootstrap sampling and copula-based Monte Carlo simulation. J. Clean. Prod., 159, 359–373. DOI: 10.1016/j.jclepro.2017.05.038

Li, B.F., Liang, X.H. and Qi, L.W.: 2011, Research on the influence of coal's uniaxial compressive strength to impact energy index. Procedia Eng., 26, 863–868. DOI: 10.1016/j.proeng.2011.11.2248

Li, X.S., Liu, Z.F. and Yang, S.: 2021, Similar physical modeling of roof stress and subsidence in room and pillar mining of a gently inclined medium-thick phosphate rock. Adv. Civ. Eng., 17. DOI: 10.1155/2021/6686981

Li, X.S., Yang, S. and Wang, Y.M.: 2021, Macro-micro response characteristics of surrounding rock and overlying strata towards the transition from open-pit to underground mining. Geofluids, 18. DOI: 10.1155/2021/5582218

Lin, P., Wei, P., Wang, C., Kang, S. and Wang, X.: 2021, Effect of rock properties on cracking and the electromagnetic radiation mechanism. J. Rock Mech. Geotech. Eng., 13, 4, 798–810. DOI: 10.1016/j.jrmge.2021.01.001

Lisjak, A. and Grasselli, G.: 2014, A review of discrete modeling techniques for fracturing processes in discontinuous rock mass. J. Rock Mech. Geotech. Eng,, 6, 301–314. DOI: 10.1016/j.jrmge.2013.12.007

Liu, T., Lin, B. and Yang, W.: 2017, Mechanical behavior and failure mechanism of pre-cracked specimen under uniaxial compression. Tectonophysics, 712/713, 330–343. DOI: 10.1016/j.tecto.2017.06.004

Liu, W.R., Wang, X. and Li, C.M.: 2019, Numerical study of damage evolution law of coal mine roadway by particle flow code (PFC) model. Geotech. Geol. Eng., 37, 4, 2883–2891. DOI: 10.1007/s10706-019-00803-6

Liu, X.X., Wu, L.X., Zhang, Y.B., Wang, S.Z., Yao, X.L. and Wu, X.Z.: 2020, The characteristics of crack existence and development during rock shear fracturing evolution. Bull. Eng. Geol. Environ., 80, 2, 1–12. DOI:10.1007/s10064-020-01997-3

Luo, D., Su, G. and Zhang, G.: 2020, True-triaxial experimental study on mechanical behaviours and acoustic emission characteristics of dynamically induced rock failure. Rock Mech. Rock Eng., 53, 10, 1205–1223. DOI: 10.1007/s00603-019-01970-x

Patil, M.S., Seo, J.H., Panchal, S. and Lee, M.Y.: 2020, Numerical study on sensitivity analysis of factors influencing liquid cooling with double cold-plate for lithium-ion pouch cell. Int. J. Energy Res., 45, 2, 2533–2559. DOI: 10.1002/er.5946

Sharafisafa, M., Aliabadian, Z. and Shen, L.: 2020, Crack initiation and failure of block-in-matrix rocks under Brazilian test using digital image correlation. Theor. Appl. Fract. Mech., 109, 102743. DOI: 10.1016/j.tafmec.2020.102743

Shirole, D., Hedayat, A., Ghazanfari, E. and Walton, G.: 2020, Evaluation of an ultrasonic method for damage characterization of brittle rocks. Rock Mech. Rock Eng., 53, 5, 2077–2094. DOI: 10.1007/s00603-020-02045-y

Sun, Z., Li, L., Wang, F. and Zhou, G.: 2019, Desorption characterization of soft and hard coal and its influence on outburst prediction index. Energ. Sources Part A Recovery Utilization and Environmental Effects, 2, 1–15. DOI: 10.1080/15567036.2019.1618991

Wang, C., Lu, Y., Shen, B., Li, Y. and Liang, Y.: 2019, Design and monitoring of CPB replacement mining RSCP: a case study in China. Energ. Sources Part A Recovery, Utilization and Environmental Effects, 43, 80–95. DOI: 10.1080/15567036.2019.1623944

Wang, R.C. and Tan, Y.L.: 2014 Experimental study on failure mechanism of soft rock roadway in Yangcheng coal. Appl. Mech. Mater., 3547, 1381–1384. DOI: 10.4028/www.scientific.net/AMM.675-677.1381

Wang, X. and Tian, L.G.: 2018, Mechanical and crack evolution characteristics of coal–rock under different fracture-hole conditions: a numerical study based on particle flow code. Environ. Earth Sci., 77, 8, 1–10. DOI: 10.1007/s12665-018-7486-3

Wang, Y., Li, X., Zhang, B. and Wu, Y.F.: 2014, Meso-damage cracking characteristics analysis for rock and soil aggregate with ct test. Sci. China Technol. Sci., 57, 7, 1361–1371. DOI: 10.1007/s11431-014-5578-1

Wong, F.S.: 1985, Slope reliability and response surface method. J. Geotech. Eng., 111, 1, 32–53. DOI: 10.1061/(ASCE)0733-9410(1985)111:1(32)

Wong, L.N.Y. and Zhang, X.P.: 2014, Size effects on cracking behavior of flaw-containing specimens under compressive loading. Rock Mech. Rock Eng., 47, 5, 1921–1930. DOI: 10.1007/s00603-013-0424-5

Xu, J. and Li, Z.: 2019, Crack propagation and coalescence of step-path failure in rocks. Rock Mech. Rock Eng., 52, 2, 965–979. DOI: 10.1007/s00603-018-1661-4

Yang, S.Q., Huang, Y.H., Tian, W.L. and Zhu, J.B.: 2017, An experimental investigation on strength, deformation and crack evolution behavior of sandstone containing two oval flaws under uniaxial compression. Eng. Geol., 217, 35–48. DOI: 10.1016/j.enggeo.2016.12.004

Yu, L., Wang, S.W., Lu, Q. and Feng, G.H.: 2016, Sensitivity analysis of existing residential building energy consumption influencing factors in cold regions. Procedia Eng., 146, 196–203. DOI: 10.1016/j.proeng.2016.06.372

Zhang, C., Wang, Y. and Jiang, T.: 2020, The propagation mechanism of an oblique straight crack in a rock sample and the effect of osmotic pressure under in-plane biaxial compression. Arab. J. Geosci., 13, 15, 1–15. DOI: 10.1007/s12517-020-05682-3

Zhang, S., Li, Y., Liu, H. and Ma, X.: 2021, Experimental investigation of crack propagation behavior and failure characteristics of cement infilled rock. Constr. Build. Mater., 268, 3, 121735. DOI: 10.1016/j.conbuildmat.2020.121735

Zhou, M., Li, Y., Wu, J., Yu, Y. and He, H.: 2020, The characteristics of high speed crack propagation at ultra high loading rate. Theor. Appl. Fract. Mech., 108, 102650. DOI: 10.1016/j.tafmec.2020.102650

Zhou, S., Zhu, H.H., Ju, J.W., Yan, Z.G. and Chen, Q.: 2017, Modeling microcapsule-enabled self-healing cementitious composite materials using discrete element method. Int. J. Damage Mech., 26, 2, 340–357. DOI: 10.1177/1056789516688835

Zhu, J.M. and Yu, H.: 2020, Analysis of crack propagation characteristics of rock-like material with double closed cracks under uniaxial compression. Geotech. Geol. Eng., 2, 6489–6509. DOI: 10.1007/s10706-020-01451-x